

Powder-Bot: A Modular Autonomous Multi-Robot Workflow for Powder X-Ray Diffraction

Amy M. Lunt, Hatem Fakhruldeen, Gabriella Pizzuto, Louis Longley, Alexander White, Nicola Rankin, Rob Clowes, Ben M. Alston, Andrew I. Cooper* and Samantha Y. Chong*

Department of Chemistry and Materials Innovation Factory, University of Liverpool, L69 3BX, UK.

E-mail: aicooper@liverpool.ac.uk, schong@liverpool.ac.uk

Abstract

Powder X-ray diffraction (PXRD) is a key technique for the structural characterisation of solid-state materials, but compared with tasks such as liquid handling, its end-to-end automation is highly challenging. This is because coupling PXRD experiments with crystallisation comprises multiple solid handling steps that include sample recovery, sample preparation by grinding, sample mounting and, finally, collection of X-ray diffraction data. Each of these steps has individual technical challenges from an automation perspective, and hence no commercial instrument exists that can grow crystals, process them into a powder, mount them in a diffractometer, and collect PXRD data in an autonomous, closed-loop way. Here we present an automated robotic workflow to carry out autonomous PXRD experiments. The PXRD data collected for polymorphs of small organic compounds is comparable to that collected under the same conditions manually. Beyond accelerating PXRD experiments, this workflow involves 13 component steps and integrates three different types of robots, each from a separate supplier, illustrating the power of flexible, modular automation in complex, multitask laboratories.

Introduction

X-ray crystallography is used routinely to characterise the structure of ordered solids,^{1,2} which is essential for building structure-function relationships for materials.^{3–5} Powder X-ray diffraction (PXRD) is particularly useful for solid-state materials characterization, and it is often easier to implement than methods that require growing and harvesting a single diffractable crystal.⁶ PXRD data can provide detailed information about the structure and purity of crystalline materials.^{7–9} It can be used for the rapid identification of different crystal forms, such as detecting the existence of polymorphs.^{10–12} This is important in materials research because different polymorphs can have different physical properties.^{13,14} More widely, polymorphism affects pharmacological activity and bioavailability in the body for pharmaceuticals.^{15,16} Pharmaceutically active molecules must undergo exhaustive screening experiments to fully understand their crystal form landscapes before they can be approved for clinical trials.^{17–19} This is time consuming and expensive, and hence methods to accelerate PXRD screening are desirable.

The use of automation and robots to carry out repetitive and iterative tasks in the lab is growing,^{20,21} but the full automation of PXRD is difficult, particularly in terms of sample preparation, because it involves powder handling. High-throughput crystallisation screens have used robotic and automated platforms,^{12,22,23} which has accelerated the discovery of materials such as pharmaceuticals,²⁴ porous cages²⁵ and photovoltaics,²⁶ but these workflows tend to be only partially automated. We must automate and connect all stages in the PXRD experiment to allow fully closed-loop workflows. This starts with crystal growth and is followed by sample preparation, which is most often mechanical grinding to reduce the crystal size to allow better orientational averaging. The resulting powders are then loaded into a sample holder, such as a multi-well plate, followed by loading the PXRD instrument and data collection. Each of these individual processes presents some technical difficulties from an automation perspective and hence it is challenging to build end-to-end automated PXRD workflows.

Here, we present a fully automated, modular robotic workflow that prepares crystalline materials and collects their powder diffraction data. This modular approach integrates three separate robotic platforms—a liquid handling and screw capping platform for the crystallization stage (Chemspeed FLEX LIQUIDOSE, Figure 1, step 1 & Supporting Information, Figures S1 & S2), a mobile manipulator for sample transport and equipment manipulation (KUKA KMR iiwa; Fig. 1, steps 1, 2, 8 & 9–12), and a dual-arm robot for sample preparation (ABB YuMi; Fig. 1, steps 3–7). The Powder-Bot workflow uses a standard Panalytical powder X-ray diffractometer, which is used by the mobile manipulator in an anthropomorphic way without any substantial modification. These heterogenous robotic and automation platforms work together synchronously to achieve the multiple steps in the workflow (Figure 1), orchestrated by our system architecture, ARChemist (Supporting Information, Figure S3).²⁷ We exemplify this workflow here with two different organic compounds and show that data collected by the autonomous Powder-Bot workflow are of comparable quality to data collected for samples prepared by hand. Hence, these data are suitable for identifying compounds and distinguishing between their polymorphs.

Description of the Powder-Bot workflow. The workflow comprises three robots and 13 integrated steps, as outlined in Figure 1 and the videos in the Supporting Information (Movies 1 & 2). First, crystals are grown using a Chemspeed platform, whereby the material of interest is dispensed in a variety of solvents or solvent mixtures and these solvents are allowed to evaporate, thus growing crystals (Step 0, not shown). Quite often this leads to large crystals that adhere strongly to the sides of the sample vials (Supporting Information, Figure S4) and these must therefore be reduced in size and removed from the vial prior to diffraction (see grinding steps, described below). In Step 1 (Fig. 1), a rack of eight crystal samples is collected from the Chemspeed platform using a mobile KUKA robotic; the Chemspeed platform was modified with an automated vertical sash door to facilitate this (Supporting Information, Figure S1). Each of the 8 vials is capped with a sample lid that contains an adhesive Kapton polymer film that will ultimately receive the ground crystalline powder, as described

below (Supporting Information, Figures S4 & S5). In Step 2, the mobile KUKA manipulator delivers the rack of 8 samples to the preparation station, which involves a dual-arm ABB YuMi robot. In Step 3, the dual-arm YuMi robot transfers the 8 samples to grinding station 1, where they are reduced in size using mechanical attrition by magnetic stirring with preloaded Teflon stir bars.

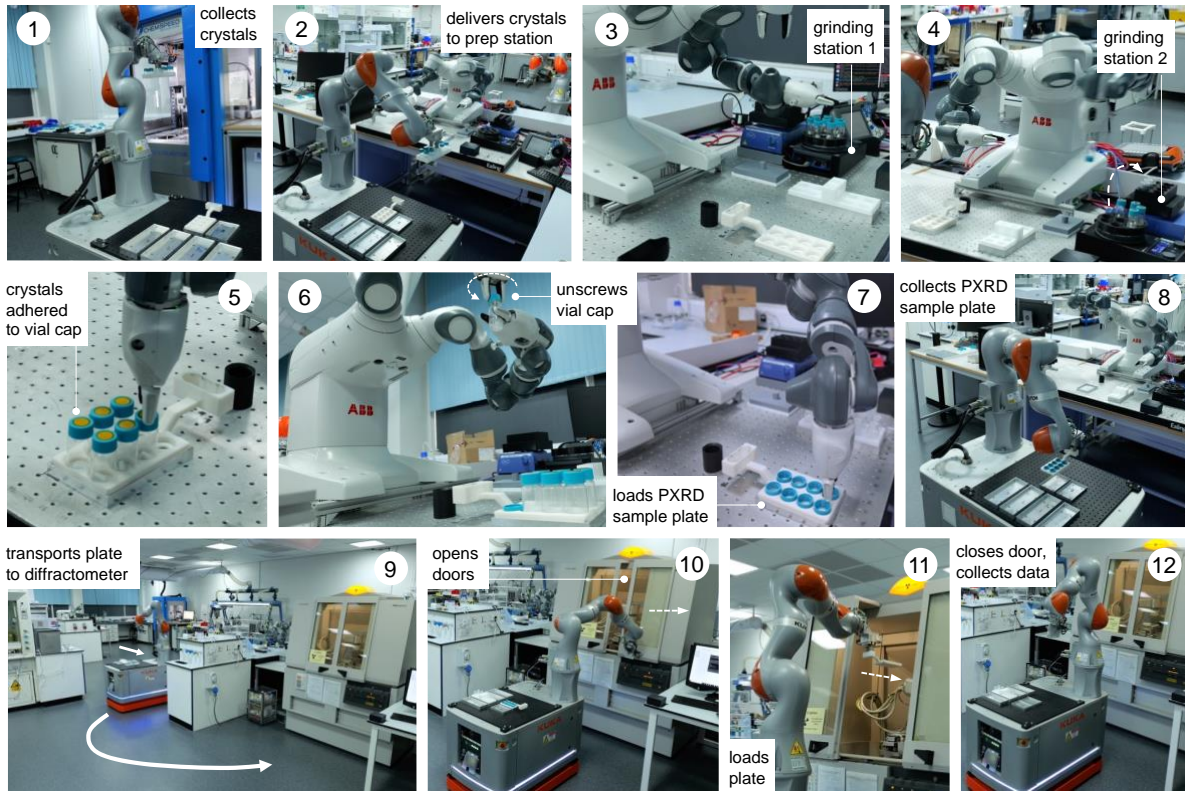


Figure 1: Workflow for the autonomous crystal growth, sample preparation and powder X-ray diffraction. The overall workflow comprises 13 separate steps and integrates three separate robots, orchestrated by our autonomous robotic chemist (ARChemist) system architecture.

In Step 4, the YuMi robot inverts the 8 samples and transfers them to grinding station 2, where they are agitated using a shaker plate to reduce the particle size further and to transfer the sample onto the adhesive Kapton polymer film in each vial's cap. In Step 5, the YuMi robot inverts the samples again and transports the samples to the X-ray diffraction plate; at this point, the sample is adhered to the vial cap (Supporting Information, Figure S4) and any excess sample and the Teflon stir bar falls back into the vial. In Step 6, the YuMi robot unscrews each vial cap, inverts it, and places it back into the PXRD plate (Step 7, see also Supporting Information, Figure S6), which is then collected by the KUKA KMR iiwa robot (Step 8) and transported to the diffractometer (Step 9). In Step 10, the KUKA robot opens the sliding doors of the diffractometer, loads the plate into the instrument (Step 11), and then closes the doors and X-ray data is collected for the 8 samples (Step 12). The sample rack can then be retrieved from the PXRD instrument and another rack of 8 samples processed and analysed, as required. A full loop of sample preparation, transport, and data collection takes around 9 hours for a rack of 8 samples.

with the data acquisition settings used here, although this time depends on the scan parameters (*i.e.*, 1 hour sample processing plus $8 \times$ 1-hour scans). The overall workflow is best appreciated from the videos supplied in the Supporting Information (Movies 1 & 2) and the associated process flow diagrams (Figures S7 & S8). As shown in Figure 2, this autonomous PXRD workflow is part of a larger laboratory that also contains several other workflows—for example, our autonomous photocatalysis workflow²⁸ is in the same area as the X-ray diffractometer (labelled **C** in Figure 2). The layout of the workflow is, to some extent, arbitrary: for example, the position of the X-ray diffractometer is fixed by proximity to its cooling water supply, and there was no space to locate the Chemspeed FLEX LIQUIDOSE robot (**A**, Figure 2) or the ABB YuMi preparation station (**B**) directly next to the diffractometer. This does not matter under a modular paradigm that uses a mobile manipulator to integrate stations because the transport time between the stations is a very small fraction of the overall workflow cycle time, as compared to the slow steps, which in this case are solvent evaporation for crystallisation and PXRD data acquisition. Moreover, this approach is scalable. For example, one can envisage coupling two workflows together, whereby the most crystalline materials are selected for testing as photocatalysts²⁸ and those powders transferred automatically into that workflow, which is housed in the same laboratory (yellow shaded area in Figure 2). Also, because we use collaborative robots, or ‘cobots’, the laboratory space can be shared with human researchers.

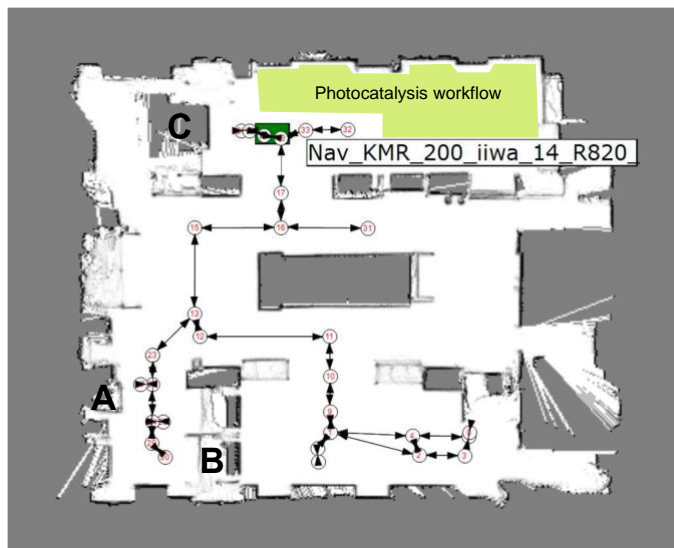


Figure 2: Modular integration of multiple robots and laboratory equipment. Image from the KUKA Sunrise OS showing the robot-generated map of the lab with numbered nodes and edges that correspond to taught paths and way points. For the experiments described here, the key modules are the Chemspeed liquid handling platform (**A**), the YuMi dual-arm sample preparation station (**B**) and the powder X-ray diffractometer (**C**). The KUKA KMR iiwa robot is shown in green, in this case approaching the X-ray diffractometer, **C**. The location of our photocatalysis workflow²⁸ (not discussed here) is shaded yellow.

Automated data collection of benzimidazole

Benzimidazole is an organic heterocyclic compound that typically exists as the alpha polymorph and takes the form of solid white crystals. Benzimidazole derivatives are used in pharmaceuticals such as antacids, antiparasitic drugs and opioids.²⁹⁻³¹ It was selected here as an initial test compound due its high solubility and low toxicity. A stock solution of benzimidazole in methanol (0.1 g/mL) was used for the automated experiment. The input station in the Chemspeed FLEX LIQUIDOSE platform was loaded with a rack of 8 sample vials (20 mL vial volume) preloaded with magnetic Teflon stir bars and capped with Kapton film vial lids, as described above. The stock solutions were dispensed into the 8 sample vials and left to evaporate inside the Chemspeed platform. After the solvent had evaporated and dry solid samples remained, the vials were capped by the Chemspeed platform. Depending on the crystallization conditions, benzimidazole often crystallizes as large, blocky crystals that are hard to recover and unsuitable for PXRD analysis without further preparation (Supporting Information, Fig. S4).

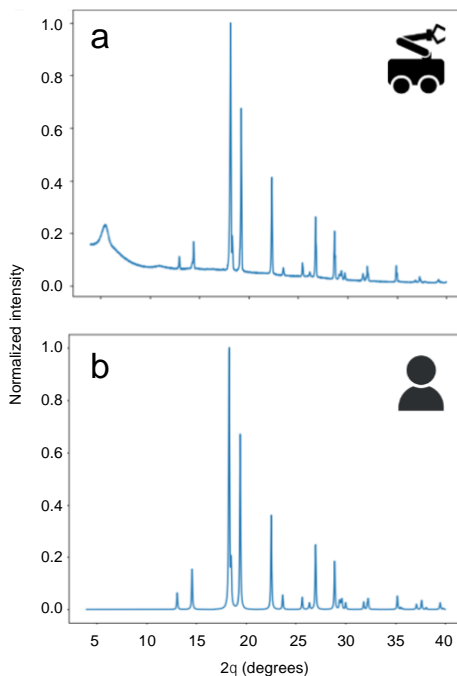


Figure 3: Comparison of powder X-ray diffraction patterns for samples prepared by robots and by humans. (a) Data collected using the autonomous robotic workflow (crystallization, grinding, and sample mounting) for the alpha polymorph of benzimidazole and (b) data collected by conventional manual methods including grinding using a pestle and mortar. Both datasets were collected in transmission mode over the range 4 to 40 in two theta in approximately 0.013 degree steps over 60 minutes.

Next, the mobile KUKA manipulator collects the samples from the Chemspeed platform and delivers them to the preparation station for and processed, as outlined above, followed by automated PXRD analysis. To compare our autonomous method with the traditional manual approach, 2 mL of the stock

solution was also dispensed into a sample vial and left to evaporate, whereafter the solid was recovered and ground manually using a mortar and pestle and mounted by hand in a 96-well aluminium plate prior to data collection. The data collected for robot-prepared and human-prepared benzimidazole crystals characterized using the same scan parameters are compared in Figure 3. The broad peak around 6° seen in the robot-collected data results from the adhesive Kapton tape on which the robot-prepared samples are loaded. Apart from that artefact, the two datasets are comparable in terms of peak width, peak positions, and relative peak intensities, suggesting that the autonomous robotic workflow has matched manual human performance for the relatively complex multistep process of sample grinding, sample recovery and sample mounting.

Automated data collection for 5-methyl-2- [(2-nitrophenyl) amino]-3-thiophenecarbonitrile (ROY)

A well-known example of an organic molecule with many polymorphs is 5-methyl-2- [(2-nitrophenyl) amino]-3-thiophenecarbonitrile, commonly referred to as ROY.³²⁻³⁵ It is an intermediate in the synthesis of the antipsychotic drug olanzapine and it is named ROY because of its red, orange and yellow polymorphs. There have been many crystallisation studies conducted for ROY, and various differently coloured polymorphs have been observed, which often occur concomitantly with each other as mixtures.³²⁻³⁵ Here, samples of ROY were prepared from solid 5-methyl-2-[(2-nitrophenyl) amino]-3-thiophenecarbonitrile by dissolving it in acetone with the addition of different percentage volumes of water as an antisolvent (Supporting Information, Table S1). In this case, the samples were prepared manually because of the slow evaporation time for water, which would require the Chemspeed robot to be idle over long periods of time, although in principle this step could have been automated as was done for benzimidazole, above. After a solid, dry product had formed, the samples were loaded into the input station for the workflow for processing and PXRD analysis, as before. This experiment produced two different polymorphs of ROY, and the data obtained by the robot was of sufficient quality to assign them easily, even when appearing as a mixture (*e.g.*, sample 4 in Figure 4c, d). The reproducibility across the batch of eight samples can also be seen in Figure 4.

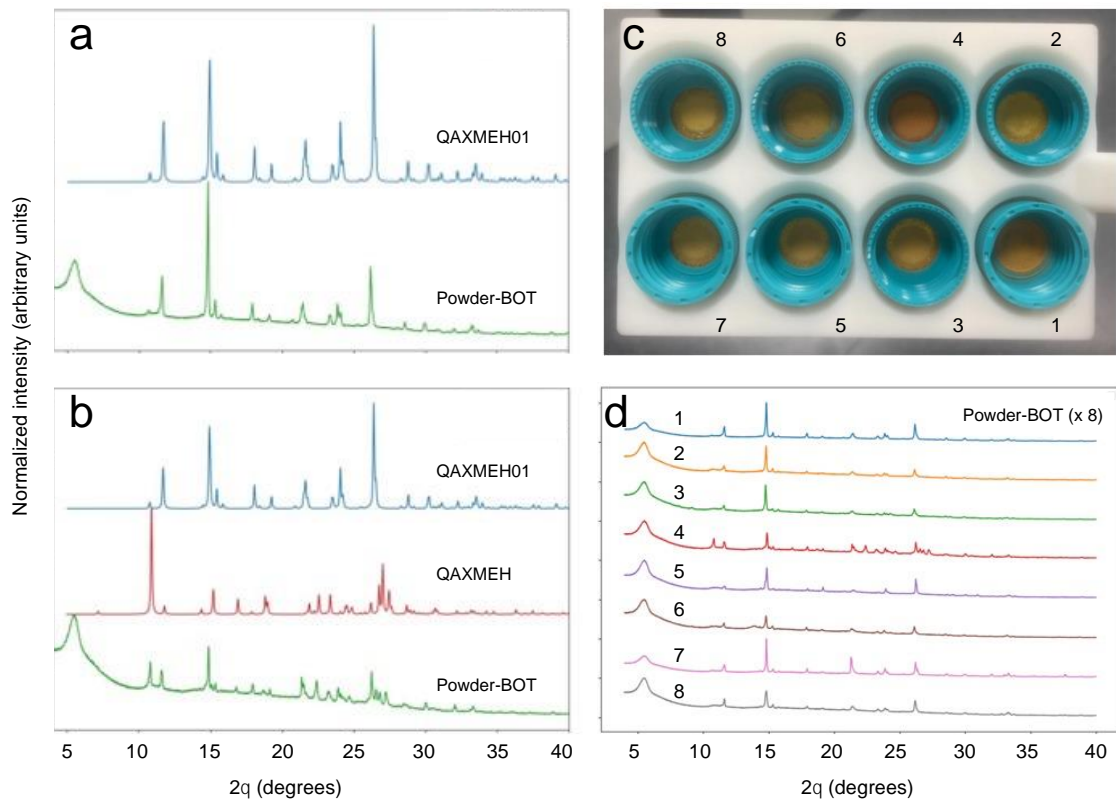


Figure 4: PXRD patterns collected for 5-methyl-2-[(2-nitrophenyl) amino]-3-thiophenecarbonitrile (ROY), as crystallized under various conditions and prepared and collected autonomously. (a) Comparison of the diffraction pattern for ROY processed using the robotic workflow (sample 1 in Fig. 4c,d; 25 mg/mL in 20:80 v/v water / acetone), as compared with the simulated PXRD pattern for the published monoclinic yellow (Y) polymorph (CSD reference code QAXMEH); (b) PXRD patterns for ROY processed using the autonomous robotic workflow (sample 4 in Fig. 4c,d; 10 mg/mL in 40:60 v/v water / acetone), as compared with the simulated patterns for two published forms: the monoclinic Y polymorph (QAXMEH) and the monoclinic orange needle (ON) polymorph (QAXMEH01); these data suggest that a phase mixture is formed under these conditions; (c) Photograph of ROY processed using the robotic workflow at various concentrations (10 or 25 mg/mL) in water / acetone mixtures (20–80% v/v water; see Supplementary Information, Table S1, for full conditions); (d) Diffraction patterns for the ROY samples shown in Fig. 4c.

Discussion

This work illustrates the potential of flexible and modular robots³⁶ to accelerate PXRD experiments and to integrate a key materials characterisation method into an automated laboratory workflow. While the videos presented in the Supporting Information show a single cycle (one rack of 8 samples), it should be possible with certain improvements to robustness to operate this workflow 24/7 over extended periods in a closed-loop way, as demonstrated in our earlier implementation of mobile robots for photocatalyst optimisation.²⁸ The introduction of sample processing and the use of three separate robots

rather than one makes this new workflow significantly more complex than our earlier study. Indeed, it ranks among the most complex autonomous systems reported for chemistry or materials research to date.^{37,38} One automated materials platform of comparable complexity is AMANDA,³⁹ which is being developed for photovoltaics research; another impressive example is the AutoBASS platform that can assemble up to 64 CR2023 battery cells.⁴⁰ However, both of those platforms involve large, custom-built integrated robotic systems. By contrast, apart from the custom-built grinding stations (a standard stir plate and a shaker, respectively, Figure 1), Powder-BOT uses robots and other laboratory hardware with little or no modification. That is, the Chemspeed FLEX LIQUIDOSE platform, the KUKA KMR iiwa robot, the dual-arm ABB YuMi robot, the IKA stirrer hotplate, the IKA shaker plate, and the Panalytical X-ray diffractometer are all ‘off the shelf’ items. Moreover, because we use a mobile manipulator to integrate the various stations, the workflow can be arranged in almost any configuration and it is easily extended by adding other stations, subject only to available laboratory space (Figure 2). As such, we see the general concept of integrating stationary and mobile robots with a modular system architecture²⁷ as a powerful strategy for automating a range of research activities beyond PXRD, driven by computational predictions, active learning, and artificial intelligence.⁴¹ To give just one example, it might be possible to use the Powder-BOT workflow to identify crystallisation conditions that produce crystalline forms that are predicted computationally to have certain desirable functional properties, and then to automatically take those materials forward for property testing.⁴²

Acknowledgements

This project has received funding from the European Research Council under the European Union's Horizon 2020 research and innovation program (grant agreement no. 856405). The authors also received funding from the Engineering and Physical Sciences Research Council (EPSRC) (EP/V026887/1, EP/T031263/1) and the Leverhulme Trust via the Leverhulme Research Centre for Functional Materials Design. AIC thanks the Royal Society for a Research Professorship (RSRP\S2\232003).

References

1. Bunaciu, A. A., Gabriela Udriștioiu, E. & Aboul-Enein, H. Y. X-ray diffraction: Instrumentation and applications. *Crit. Rev. Anal. Chem.* **45**, 289–299 (2015).
2. Sedigh Rahimabadi, P., Khodaei, M. & Koswattage, K. R. Review on applications of synchrotron-based X-ray techniques in materials characterization. *X-Ray Spectrom.* **49**, 348–373 (2020).
3. Hasell, T. *et al.* Porous organic alloys. *Angew. Chem., Int. Ed.* **51**, 7154–7157 (2012).

4. Shields, C. E. *et al.* Experimental confirmation of a predicted porous hydrogen-bonded organic framework. *Angew. Chemie Int. Ed.* e202303167 (2023).

5. Censi, R. & Di Martino, P. Polymorph impact on the bioavailability and stability of poorly soluble drugs. *Molecules* **20**, 18759 (2015).

6. Harris, K. D. M. & Cheung, E. Y. How to determine structures when single crystals cannot be grown: opportunities for structure determination of molecular materials using powder diffraction data. *Chem. Soc. Rev.* **33**, 526–538 (2004).

7. Harris, K. D. M., Tremayne, M. & Kariuki, B. M. Contemporary advances in the use of powder X-ray diffraction for structure determination. *Angew. Chem., Int. Ed.* **40**, 1626–1651 (2001).

8. Černý, R. Crystal structures from powder diffraction: Principles, difficulties and progress. *Crystals* **7**, 142 (2017).

9. Holder, C. F. & Schaak, R. E. Tutorial on powder X-ray diffraction for characterizing nanoscale materials. *ACS Nano* **13**, 7359–7365 (2019).

10. Yao, X., Henry, R. F. & Zhang, G. G. Z. Ritonavir Form III: A new polymorph after 24 years. *J. Pharm. Sci.* **112**, 237–242 (2023).

11. Li, J., Bourne, S. A. & Caira, M. R. New polymorphs of isonicotinamide and nicotinamide. *Chem. Commun.* **47**, 1530–1532 (2011).

12. Rosso, V. W. *et al.* High-throughput crystallization screening technique with transmission PXRD analysis. *Org. Process Res. Dev.* **27**, 1437–1444 (2023).

13. Hasell, T., Schmidtmann, M. & Cooper, A. I. Molecular doping of porous organic cages. *J. Am. Chem. Soc.* **133**, 14920–14923 (2011).

14. Zhang, P. *et al.* Polymorphism, phase transformation and energetic properties of 3-nitro-1,2,4-triazole. *RSC Adv.* **8**, 24627–24632 (2018).

15. Morissette, S. L., Soukasene, S., Levinson, D., Cima, M. J. & Almarsson, Ö. Elucidation of crystal form diversity of the HIV protease inhibitor ritonavir by high-throughput crystallization. *Proc. Natl. Acad. Sci. U. S. A.* **100**, 2180–2184 (2003).

16. Lee, E. H. A practical guide to pharmaceutical polymorph screening & selection. *Asian J. Pharm. Sci.* **9**, 163–175 (2014).

17. Morissette, S. L. *et al.* High-throughput crystallization: Polymorphs, salts, co-crystals and solvates of pharmaceutical solids. *Adv. Drug Deliv. Rev.* **56**, 275–300 (2004).

18. Alvarez, A. J., Singh, A. & Myerson, A. S. Polymorph screening: Comparing a semi-automated approach with a high throughput method. *Cryst. Growth Des.* **9**, 4181–4188 (2009).

19. Newman, A. Specialized solid form screening techniques. *Org. Process Res. Dev.* **17**, 457–471 (2013).

20. Nikolaev, P. *et al.* Autonomy in materials research: A case study in carbon nanotube growth. *npj Comput. Mater.* **2**, (2016).

21. Kong, F., Yuan, L., Zheng, Y. F. & Chen, W. Automatic liquid handling for life science: a critical review of the current state of the art. *J. Lab. Autom.* **17**, 169–185 (2012).

22. Florence, A. J., Johnston, A., Fernandes, P., Shankland, N. & Shankland, K. An automated platform for parallel crystallization of small organic molecules, *J. Appl. Cryst.*, **39**, 922–924 (2006).

23. Brown, C. J. *et al.* Enabling precision manufacturing of active pharmaceutical ingredients: workflow for seeded cooling continuous crystallisations. *Mol. Syst. Des. Eng.* **3**, 518–549 (2018).

24. Peterson, M. L. *et al.* Iterative high-throughput polymorphism studies on acetaminophen and an experimentally derived structure for form III. *J. Am. Chem. Soc.* **124**, 10958–10959 (2002).

25. Greenaway, R. L. *et al.* High-throughput discovery of organic cages and catenanes using computational screening fused with robotic synthesis. *Nat. Commun.* **2018** *9*, 1–11 (2018).

26. Li, Z. *et al.* Robot-accelerated perovskite investigation and discovery. *Chem. Mater.* **32**, 5650–5663 (2020).

27. Fakhruldeen, H., Pizzuto, G., Glowacki, J. & Cooper, A. I. ARChemist: Autonomous Robotic Chemistry System Architecture. *Proc. IEEE Int. Conf. Robot. Autom.* 6013–6019 (2022).

28. Burger, B. *et al.* A mobile robotic chemist. *Nature*, **583**, 237–241 (2020).

29. Lee, Y. T., Tan, Y. J. & Oon, C. E. Benzimidazole and its derivatives as cancer therapeutics: The potential role from traditional to precision medicine. *Acta Pharm. Sin. B* **13**, 478 (2023).

30. Zieliński, W. & Katrusiak, A. Hydrogen bonds NH···N in compressed benzimidazole polymorphs. *Cryst. Growth Des.* **13**, 696–700 (2013).

31. Krawczyk, S. & Gdaniec, M. Polymorph β of 1H-benzimidazole. *Acta Crystallogr. Sect. E Struct. Reports Online* **61**, o4116–o4118 (2005).

32. Yu, L. *et al.* Thermochemistry and conformational polymorphism of a hexamorphic crystal system. *J. Am. Chem. Soc.*, **122**, 585–591 (2000).

33. Chen, S., Guzei, I. A. & Yu, L. New polymorphs of ROY and new record for coexisting polymorphs of solved structures. *J. Am. Chem. Soc.* **127**, 9881–9885 (2005).

34. Tan, M. *et al.* ROY revisited, again: the eighth solved structure. *Farad. Discuss.*, **11**, 477–491 (2018).

35. Yu, L. Polymorphism in molecular solids: An extraordinary system of red, orange, and yellow crystals. *Acc. Chem. Res.* **43**, 1257–1266 (2010).

36. MacLeod, B.P., *et al.* Flexible automation accelerates materials discovery. *Nat. Mater.* **21**, 722–726 (2022).

37. Steiner, S. *et al.* Organic synthesis in a modular robotic system driven by a chemical programming language. *Science*, **363**, eaav2211 (2019).

38. B. P. MacLeod *et al.* Self-driving laboratory for accelerated discovery of thin-film materials. *Sci. Adv.* **6**, eaaz8867 (2020).

39. Wagner, J., *et al.* The evolution of Materials Acceleration Platforms: toward the laboratory of the future with AMANDA. *J. Mater. Sci.*, **56**, 16422–16446 (2021).

40. Zhang, B., Merker, L., Sanin, A. & Stein, H. S. Robotic cell assembly to accelerate battery research. *Digital Discovery*, **1**, 755–762 (2022).

41. Ren, Z., Ren, Z., Zhang, Buonassisi, T. & Li, J. Autonomous experiments using active learning and AI. *Nat. Rev. Mater.* **8**, 563–564 (2023).

42. Pulido, A., *et al.* Functional materials discovery using energy–structure–function maps. *Nature*, **543**, 657–664 (2017)

Powder-Bot: A Modular Autonomous Multi-Robot Workflow for Powder X-Ray Diffraction

Amy. M. Lunt, Hatem Fakhruldeen, Gabriella Pizzuto, Louis Longley, Alexander White, Nicola Rankin, Rob Clowes, Ben Alston, Andrew I. Cooper* and Sam. Y. Chong*

Supporting Information

Movie 1 (6 min 16 sec, recorded at 4K resolution): Captioned video overview of the 12 stages of the autonomous PXRD workflow described in Fig. 1 in the main paper as associated text. Note that the video is accelerated by varying degrees at different stages of the workflow, but the average acceleration is approximately x 10. An unaccelerated version of this movie without captions (55 min 29 sec) is included below.

YouTube link: <https://youtu.be/8rnaoTF-VMk>

Original video file (downloadable):

https://www.dropbox.com/s/riq3jktroa74dbs/PXRD_6%27_16%22_captions_4K.mp4?dl=0

Movie 2 (55 min 29 sec, recorded at 4K resolution): Video showing full workflow run including sample processing, transport, and PXRD data acquisition with no acceleration and no captions. Note that neither of these movies shows the initial sample preparation step (liquid dispensing and evaporation) that is carried out by the Chemspeed platform (Figures S1 & S2) prior to grinding, sample mounting and PXRD analysis; both videos start at the point where crystals have already been grown.

YouTube link: <https://youtu.be/cKAELaBfqEI>

Original video file (downloadable):

https://www.dropbox.com/s/x2xoej9cceovczk/Amy_WF_full_54%27_29_no_captions.mp4?dl=0

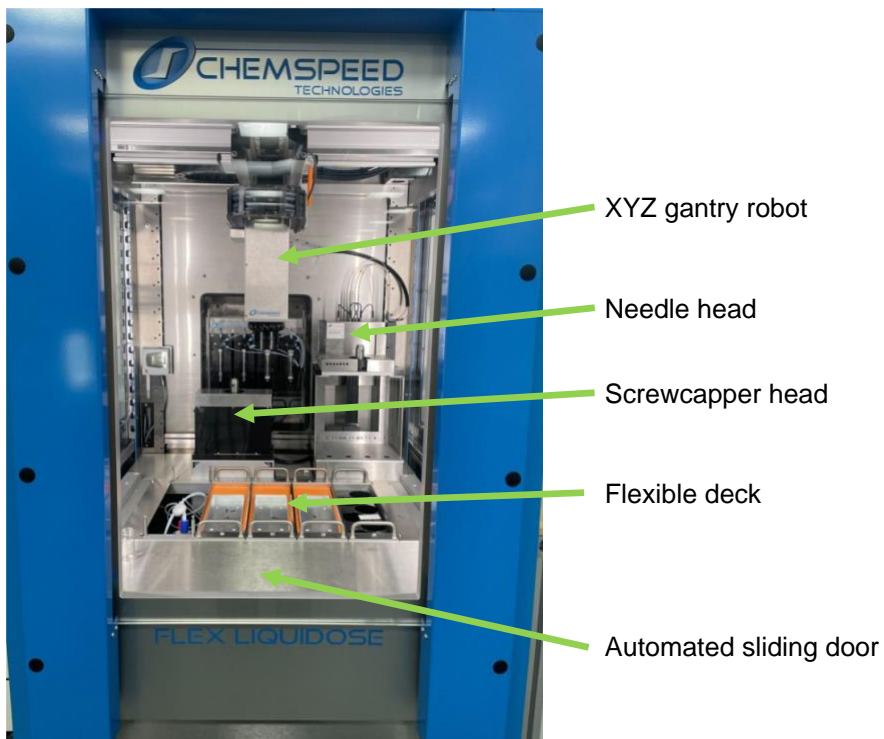


Figure S1: Chemspeed FLEX LIQUIDOSE platform, highlighting the vertical automated sliding door (a bespoke adaptation for this project), the interchangeable needle and screwcapper heads, the flexible deck layout, and the XYZ gantry robot for sample transport.

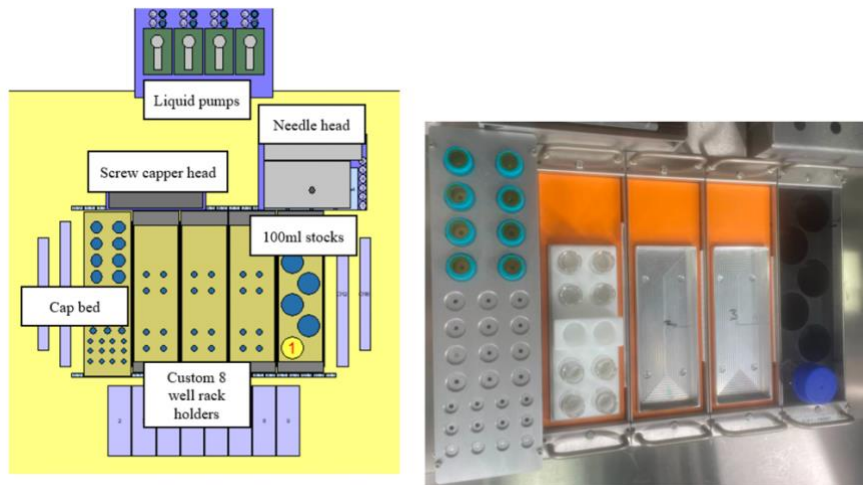


Figure S2: Left: Screenshot of the deck layout of the workflow, taken from the AutoSuite software. Right: Photograph of the equivalent deck layout in the Chemspeed FLEX LIQUIDOSE platform, with one occupied and two empty 8-vial racks. The Kapton-film vial caps are preloaded in the rack on the left.

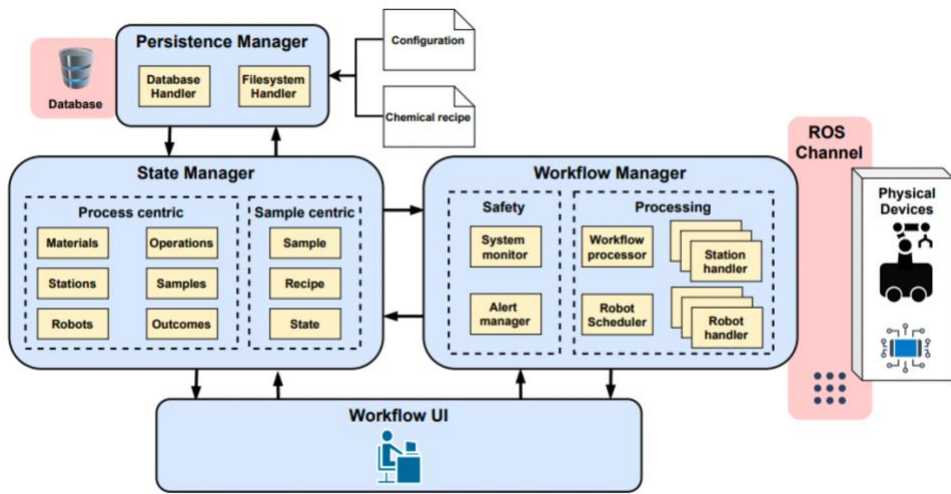


Figure S3: Block diagram summary of ARChemist software used to orchestrate the workflow (ref. 27, main text). The *State Manager* is responsible for representing the chemistry experiment state. The *Persistence Manager* allows the storage and retrieval of this state from a database and is responsible for parsing the input files. The *Workflow Manager* processes the experiment samples and assigns them to their respective robots and stations. The architecture uses ROS as a communication layer to interact with the physical robots and lab equipment. The *Workflow User Interface* allows the scientist to interact with the system and provide their input.

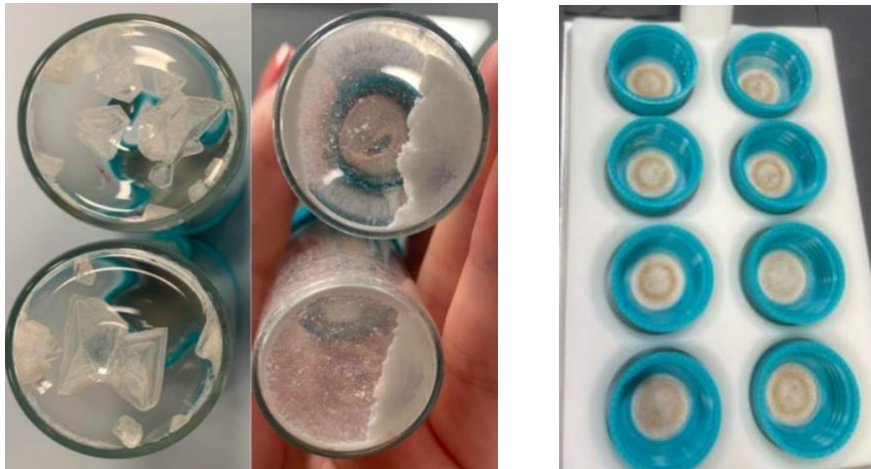


Figure S4: Left: Photograph comparing typical benzimidazole crystals as grown from methanol by evaporation in a glass vial (which are strongly adhered to the vial wall) with the same samples after automated grinding, which consisted of two minutes stirring and two minutes shaking with a standard magnetic stirrer in each vial (Steps 3 & 4 in Figure 1, main text). Right: Photograph showing the PXRD plate after robotic sample preparation of the

benzimidazole crystals. The plate contains the 8 caps, each with an adhesive Kapton tape film (Figure S5). As described in Figure 1 and main text (see also Movie 1), the robotic workflow has reduced the particle size of the large benzimidazole crystals and grinding station 2 (see Steps 4 & 5 in Figure 1, main text) has coated each film with a light dusting of the powdered benzimidazole material, which adheres to the Kapton tape.

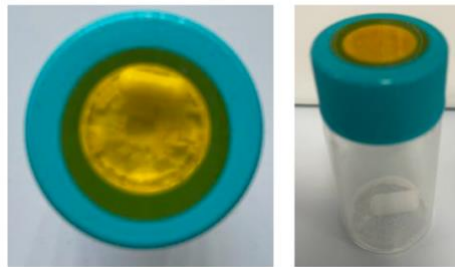


Figure S5: Photograph showing glass sample vials with a Kapton film covering the septum vial cap. The adhesive side of the Kapton film faces into the sample vial.

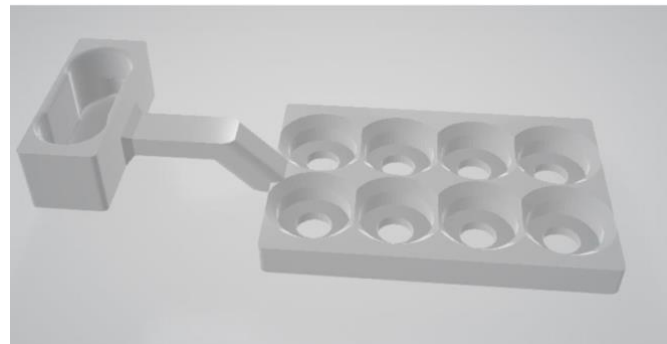
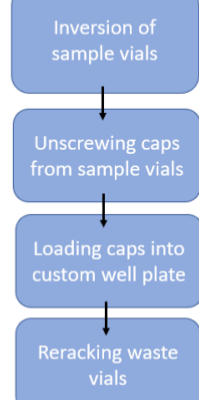
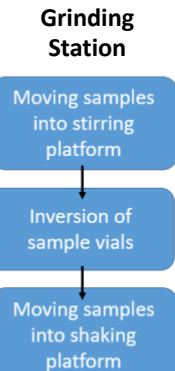


Figure S6: Design for the final prototype of the PXRD sample plate substrate, which includes a custom handle that is complementary to the robot end effectors (see e.g., manipulations in **Movie 1**, 4 min 20 sec and 5 min 12 sec). The same design for robot grasping was also used for the sample transport plate (see 0 min 13 sec in **Movie 1**). The sample holes are chamfered to allow easy loading of the sample caps.

Crystallisation Station



Sample Preparation Station



Data Collection Station

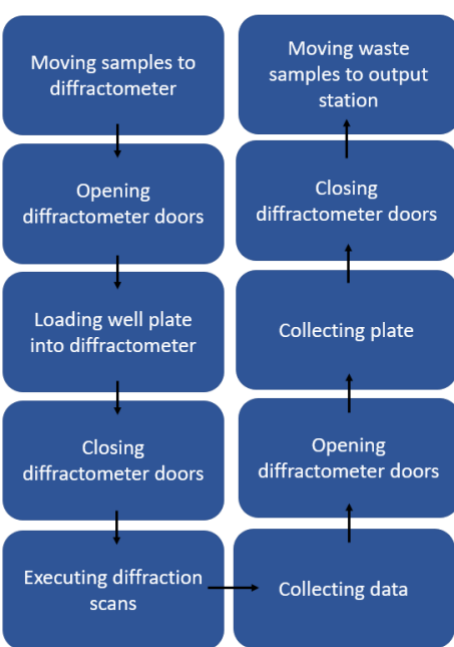


Figure S7: Flow diagram summarizing the various steps in the workflow.

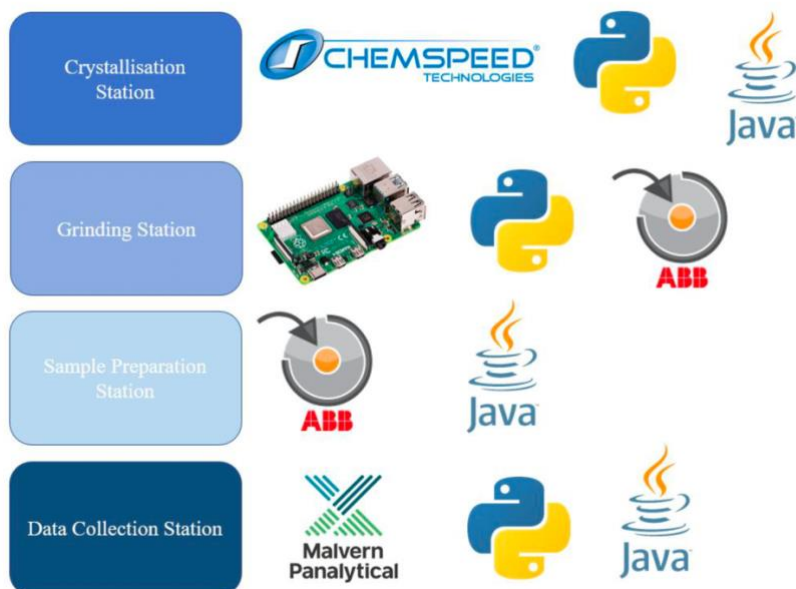


Figure S8: Overview of the control protocols and programming languages used for each station in the workflow. The images depict Chemspeed Autosuite GUI, Python programming language, Java programming language, Raspberry Pi microcontroller, ABB RobotStudio GUI and Malvern Panalytical GUI.

```

[ShakerPlateStation_22]: Current state changed to StationState.WAITING_ON_ROBOT
[WorkflowManager]: KukaLBRTask with task: UnloadPXDRackYumiStation, params: ['True'] @(30, 1) is added to robot scheduling queue.
[KukaLBRIIWA_1]: Job (KukaLBRTask with task: UnloadPXDRackYumiStation, params: ['True'] @(30, 1)) is assigned.
[KukaLBRIIWA_1]: Current state changed to RobotState.OP_ASSIGNED
[KukaLBRIIWA_1]: Job (KukaLBRTask with task: UnloadPXDRackYumiStation, params: ['True'] @(30, 1)) is retrieved.
[KukaLBRIIWA_1]: Current state changed to RobotState.IDLE
[WorkflowManager]: KukaLBRIIWA_1 finished executing job KukaLBRTask with task: UnloadPXDRackYumiStation, params: ['True'] @(30, 1)
[WorkflowManager]: Notifying ShakerPlateStation_22
[ShakerPlateStation_22]: Robot job request is fulfilled.
[ShakerPlateStation_22]: Current state changed to StationState.PROCESSING
[ShakerPlateStation_22]: Robot job request for (KukaLBRTask with task: UnloadEightWRackYumiStation, params: ['False'] @(30, 1)) is retrieved.
[ShakerPlateStation_22]: Current state changed to StationState.WAITING_ON_ROBOT
[WorkflowManager]: KukaLBRTask with task: UnloadEightWRackYumiStation, params: ['False'] @(30, 1) is added to robot scheduling queue.
[KukaLBRIIWA_1]: Job (KukaLBRTask with task: UnloadEightWRackYumiStation, params: ['False'] @(30, 1)) is assigned.
[KukaLBRIIWA_1]: Current state changed to RobotState.OP_ASSIGNED
[KukaLBRIIWA_1]: Job (KukaLBRTask with task: UnloadEightWRackYumiStation, params: ['False'] @(30, 1)) is retrieved.
[KukaLBRIIWA_1]: Current state changed to RobotState.IDLE
[WorkflowManager]: KukaLBRIIWA_1 finished executing job KukaLBRTask with task: UnloadEightWRackYumiStation, params: ['False'] @(30, 1)
[WorkflowManager]: Notifying ShakerPlateStation_22
[ShakerPlateStation_22]: Robot job request is fulfilled.
[ShakerPlateStation_22]: Current state changed to StationState.PROCESSING

[KukaLBRIIWA_1]: Job (KukaLBRTask with task: LoadPXDRackYumiStation, params: ['False'] @(30, 1) is complete.
[KukaLBRIIWA_1]: Current state changed to RobotState.EXECUTION_COMPLETE
[IkaPlateDigital_23]: Requesting robot job (YuMiRobotTask with task: loadIKAPlate, params: [] @(30, 1))
[IKASTirPlateSm]: current state is load_stir_plate
[YuMiRobot_123]: Current state changed to RobotState.EXECUTING_OP
[INFO] [1684325354.275454]: executing loadIKAPlate
[YuMiRobot_123]: Job (YuMiRobotTask with task: loadIKAPlate, params: [] @(30, 1) is complete.
[YuMiRobot_123]: Current state changed to RobotState.EXECUTION_COMPLETE
[IkaPlateDigital_23]: Current state changed to StationState.OP_ASSIGNED
[IkaPlateDigital_23]: Requesting station job (<archemist.stations.ika_digital_plate_station.state.IKASTirPlateDescriptor object at 0x7ff86408e7430>)
[IKASTirPlateSm]: current state is stir
[IkaPlateDigital_23]: Current state changed to StationState.EXECUTING_OP
[INFO] [1684325396.002056]: executing stirring operation
[IkaPlateDigital_23]: Station op is complete.
[IkaPlateDigital_23]: Current state changed to StationState.PROCESSING

```

Figure S9: Two screenshots showing examples of the command line interface where the ARChemist server is launched (upper) and command line interface for the Handlers execution logs (lower). See Figure S3 for the general ARChemist overview.

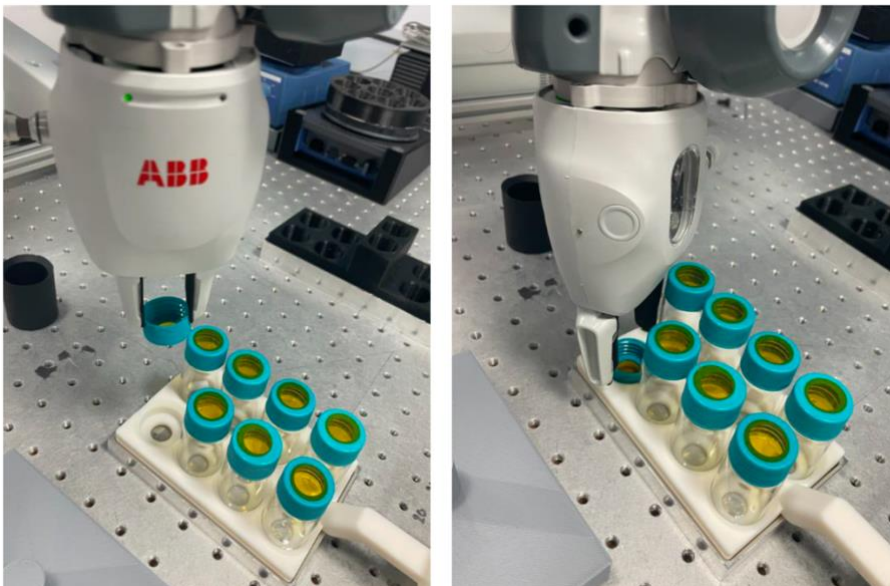


Figure S10: Photograph showing ABB YuMi robot placing a sample cap into the PXRD sample holder (Figure S3. In this case the vials are unloaded; when loaded with sample, the Kapton film becomes opaque (see e.g., **Movie 1**, 2 min 40 sec *et seq.*).

```
! unscrew
FOR i FROM 1 TO 8 DO
    g_GripIn \holdForce:=10;
    MoveL RelTool (CRobT(\Tool:=GripperR),0,0,-1,\Rz:=-95), v200, z50,GripperR;
    WaitRob \ZeroSpeed;
    g_GripOut \holdForce:=10;
    MoveL RelTool (CRobT(\Tool:=GripperR),0,0,0,\Rz:=95), v200, z50,GripperR;
    WaitRob \ZeroSpeed;
ENDFOR
```

Figure S11: Code snippet from ABB RobotStudio software used to unscrew vial caps with the YuMi robot (see Step 6 in Figure 1, main text, also **Movie 1**, 2 min 49 sec *et seq.*).

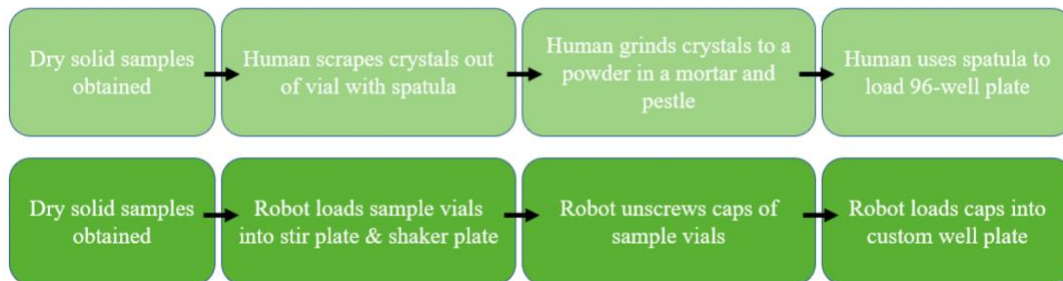


Figure S12: Schemes comparing typical human workflow (top) and autonomous robot workflow (bottom) for PXRD sample preparation.

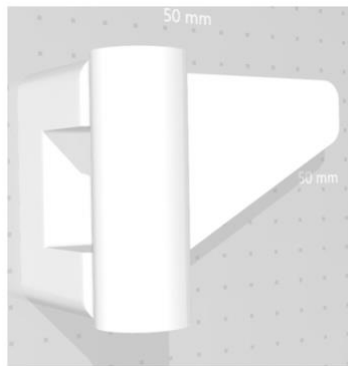


Figure S13: CAD file for handles modifications for the X-ray diffractometer; the triangular insert fits into a recess in the diffractometer doors, and this was the only physical modification to the X-ray diffractometer, allowing the robot to open and close these doors reliably (**Movie 1**, 4 min 52 sec *et seq.*) using the same end effector as used to manipulate the sample holders. We

note that the KUKA robot was able to operate the diffractometers without any modification by using the existing recessed handles, but this simple modification made the process smoother and more robust.

Sample number	Concentration of ROY in acetone (mg/mL)	Percentage of water in the crystallisation solution (% v/v)
1	25	20
2	25	60
3	25	50
4	10	40
5	10	50
6	10	70
7	10	80
8	10	30

Table S1: ROY samples were prepared in 20 mL glass vials at a total solution volume of 3 mL and left to evaporate to dryness in a fume cupboard.

Code and Driver Repositories

The full software and drivers for the workflow can be found in the following repositories:

KUKA Sunrise programs: KUKA programs from SunriseOS for the new frames for the mobile robot operations developed in this project:

https://github.com/sgalunt/Thesis_Amy_Lunt/tree/main/Appendix%201%20KUKA%20code

ABB RobotStudio programs: Full ABB programs from RobotStudio for the YuMi dual-arm robot operations:

https://github.com/sgalunt/Thesis_Amy_Lunt/tree/main/Appendix%202%20YuMi%20code

ABB YuMi dual-arm robot driver:

https://github.com/sgalunt/Thesis_Amy_Lunt/blob/main/Appendix%203%20Drivers/yumi_driver.py

IKA stir plate driver:

https://github.com/sgalunt/Thesis_Amy_Lunt/blob/main/Appendix%203%20Drivers/ika_serial_driver.py

Panalytical PXRD driver:

https://github.com/sgalunt/Thesis_Amy_Lunt/blob/main/Appendix%203%20Drivers/pxrd_driver.py

ARChemist Process Files: Specifically, new files developed for this workflow:

https://github.com/sgalunt/Thesis_Amy_Lunt/tree/main/Appendix%204%20ARChemist%20code/Process%20Files

ARChemist Configuration Files:

https://github.com/sgalunt/Thesis_Amy_Lunt/tree/main/Appendix%204%20ARChemist%20code/Configuration%20Files

ARChemist Recipe Files:

https://github.com/sgalunt/Thesis_Amy_Lunt/tree/main/Appendix%204%20ARChemist%20code/Recipe%20Files